ELSEVIER

Journal of Molecular Catalysis A: Chemical 119 (1997) 105–112

JOURNAL OF MOLECULAR CATALYSIS A: CHEMICAL

Structure and initial interaction of butane and butane isomers in a Pt/H-mordenite catalyst

M.E. Grillo *, M.M. Ramírez de Agudelo

INTEVEP, S.A., Research and Technological Support Center of Petróleos de Venezuela, P.O. Box 76343, Caracas 1070A, Venezuela

Received 7 July 1996; accepted 14 October 1996

Abstract

The relationship between structure and catalytic performance of Pt–HMOR model catalysts towards the *n*-butane hydroisomerization reaction is studied employing a combination of simulation strategies. The *n*-butane binding energy increases with Pt loading. This behavior is explained based on the different locations obtained of low-energy *n*-butane adsorption sites at limiting Pt loadings. At high metal loading, the effective pore blocking by large Pt particles leads to the adsorption of *n*-butane in small side pockets. The high coordination with oxygen ions at these sites offers the best stabilization through optimization of adsorbate-zeolite dispersion forces. This structural explanation for the calculated binding energy change with the increase in platinum concentration is consistent with that proposed by a previous Monte Carlo study of the relatively high heat of adsorption of methane in mordenite. The lower the metal dispersion the more strongly bound the *n*-butane is, compared to *iso*-butane and butane isomers. Pt sites associated to clusters of up to six atoms in size, located in the main channel might be energetically accessible for a single *n*-butane molecule, as suggested by the calculated migration energy profiles.

Keywords: Platinum clusters; *n*-butane hydroisomerization; Butane isomers; Bifunctional catalyst; Monte Carlo study; Molecular dynamics; Sorption simulations

1. Introduction

The bifunctional catalyst Pt/H-mordenite (Pt–HMOR) is used in refining industry for hydroisomerization of light alkane cuts. In particular, the hydroisomerization of *n*-butane produces isobutane which is an important raw material for alkylation and isobutene production (used in MTBE synthesis). Its economic importance arises from the demands of octane number enhancers in reformulated gasoline. Understanding the preparation procedure leading to the most selective catalyst is therefore of economic interest. Furthermore, the study of catalytic and adsortive performance of model Pt–HMOR system assists on catalytic process optimizations.

On acidic mordenite (HMOR), *n*-butane isomerization occurs over Brønsted acid sites in the main channel. The highest selectivity to *iso*-butane is obtained at low temperature and low acid sites concentration [1]. In a recent

* Corresponding author.

PII S1381-1169(96)00474-8

infrared spectroscopy study on the sorption of light *n*- and *iso*-alkanes on HMOR [2], solely the Brønsted acid sites in the mordenite straight channels are proposed to be accessible for alkane molecules. Furthermore, only one alkane molecule can be accommodated on these sites.

In the case of the bifunctional catalysts Pt–HMOR, *n*-butane is dehydrogenated on the metal function, the olefin so produced is isomerized on acidic sites and hydrogenated back on the metal [3]. The activity and selectivity to light isomers (i-C_{4-5}) of Pt–HMOR at 573 K using n-C_8 as feed has been found to increase with the platinum concentration [4]. Thus far, it is unknown whether the active metal site is a single atom or a platinum cluster, confined to the HMOR main channel. In the present study, computer simulation methods are applied to identify the location and structure of the active platinum sites for the hydroisomerization reaction of *n*-butane on Pt–HMOR model catalysts of different metal loading levels. A further point at issue is the effect of the metal dispersion on the relative binding energies of isomeric butanes and butenes on Pt–HMOR.

The present simulations take advantage of the principal features of molecular simulations docking strategy to address the adsorption behavior of the different hydrocarbons considered within the cavities of Pt–HMOR model host structures [5]. This procedure combines Monte Carlo (MC), molecular dynamics (MD) and energy minimization (EM) techniques. Predictions on effects of the metal dispersion upon catalytic performance are made based on the relative binding energies of the different butane and butane isomers on Pt–HMOR structures, at different metal loadings. Furthermore, the accessibility of the Pt-sites in these models was estimated calculating the energy differences along migration energy profiles of *n*-butane into the Pt–HMOR main channel. The docking strategy has already been successfully applied to simulations of hydrocarbon adsorption within zeolite framework structures, and it is described in detail in reference [6].

2. Computational procedure

The methodology used in the present study differs from the standard docking procedure in the following features: (a) the whole framework structure is relaxed during the energy minimization, and (b) only selected low energy sorbate docked structures are optimized in the minimization stage.

2.1. Sorption simulations

The discover code [7] was used to perform lattice energy minimizations (LEM) and molecular dynamics simulations (MD), utilizing interatomic potential parameters from a MSIs consistent valence force field (CVFFCALP). The adsorbate–zeolite short-range interactions are calculated with a Lennard–Jones (12-6) potential energy function to a cut-off of 9.5 Å. This force field accounts for different short-range van der Waals (vdW) forces between the hydrocarbon hydrogens and the Si–O–Si, Si–O–Al and Pt sites. The potential model used, however, does not contain parameters for the interaction of the zeolitic hydroxyl groups and the hydrocarbon CH groups. Hence, the present simulations do not account for the effect of the zeolite Brønsted acid sites on the hydrocarbon sorption behavior, and therefore only provide a qualitative estimation of the relative isomer sorption ability. The potential parameters used are presented in Table 1.

Table 1
Interatomic potential parameters, A_i and B_i, in kcal mol^{-1} Å^{12} and kcal mol^{-1} Å^6

i	A_i	B_i
C	1981049.2250	1125.9980
H	7108.4660	32.8708
O	272894.7846	498.8788
Si	3149175.0000	710.0000
Al	3784321.4254	11699.8493
Pt	4576819.9618	16963.3082

Lennart–Jones: $V(r_{ij}) = q_i q_j / r_{ij} + A_{ij} / r_{ij}^{12} - B_{ij} / r_{ij}^6$. The off-diagonal potential parameters take the form $A_{ij} = \sqrt{A_i \times A_j}$ and $B_{ij} = \sqrt{B_i \times B_j}$.

The use of a pair-wise Lennard–Jones potential is a severe approximation in the calculations. The potential energy surface used in the present work is thus not realistic. However, the success of this approximation in previous studies of the self-diffusion of metallic adsorbates on metallic substrates [8–10] and atomic C and O self-diffusion on Pt(111) [11], together with the study of the structural features of platinum deposited on a vitreous silica substrate [12], encourages the use of Lennard–Jones potentials from MSI in this work.

The conformations of the molecule to be sorbed are first sampled by molecular dynamics at 500°C. The adsorbate molecule was equilibrated for 500 iterations to the desired temperature and the dynamic was run for further 500 iterations. The MD simulations were performed at a time step of 0.001 ps in the canonical ensemble (NVT). The equations of motion are integrated using the Verlet algorithm, and the temperature was controlled by scaling particle velocities. A total number of 50 conformations of *n*-butane, and of the isomers, were extracted from the dynamics run, and were inserted in the Pt–HMOR host structures using the MC docking procedure.

The docking strategy enables an effective sampling of all possible adsorption sites within the host structure to be performed. Using this method, thirty insertion attempts into the Pt–HMOR host structure were carried out, for each of the fifty generated adsorbate conformations. The docking algorithm searches automatically for low energy host–guest structures according to an energy threshold, taking into account vdW interactions between the trial adsorbate conformation and the zeolite walls.

The last stage of the simulation procedure involves the optimization of low sorption energy structures generated from the MC docking. This step leads to the identification of active sites for *n*-butane adsorption in the Pt–HMOR models considered. The adsorbed hydrocarbon/Pt–HMOR structures are optimized by minimizing the lattice energy with respect to the whole (adsorbate + zeolite) atomic coordinates. The lattice energy is calculated and optimized using the discover program. The long-range Coulombic interactions of the mordenite lattice are calculated using periodic boundary conditions by the Ewald summation method. The quasi Newton minimization algorithm was used to a maximum derivative of 1×10^{-5}.

Regarding the selection of the host–guest energy threshold, two different sets of calculations have been performed. A first set of MC docking calculations were carried out at a threshold of 773 kcal/mol. This setting allows to consider docked structures with steric interactions. In order to find the lowest energy sorption sites in the dispersed Pt–HMOR model catalysts, a second set of MC insertions were calculated at 0 kcal/mol. This energy setting implies that only attractive van der Waals contacts between the trial adsorbate conformations and the zeolite walls are accepted as candidate structures, and therefore the accepted configurations are free of steric interactions. This allows to an effective search of low adsorption energy sites within the host structure to be performed.

The host structures consist of a mordenite unit cell containing two aluminum ions at the T1 and T3 tetrahedral sites, two charge compensating protons and a Pt cluster, $(Pt)_xH_2Al_2Si_{46}O_{96}$ (x number of Pt atoms). The starting host structures were fully relaxed prior to the hydrocarbon sorption, as described in a previous work [13]. The obtained amorphization upon relaxation of fcc Pt clusters supported in HMOR cages as well as on a vitreous silica surface has been discussed before [13,12].

Two different kinds of Pt clusters are considered regarding the metal loading level and dispersion of the Pt–HMOR model catalysts. The first type of model simulates a non-dispersed Pt–HMOR catalysts containing a metal cluster of 22 atoms in size (model 20). This model has twenty Pt atoms filling the main channel and two isolated Pt sites in the side pockets. A second kind of model is defined to simulate

highly dispersed Pt–HMOR catalysts. For this purpose, two different cluster models are considered containing 6 and 4 atoms in the main channel and isolated Pt sites in the side pockets (models 6 and 4, respectively). These models permit to address the effect of the number of available Pt sites hosted in the main channel on the hydrocarbon sorption behavior.

2.2. *n*-butane migration into Pt–HMOR

In order to assess the accessibility of Pt sites in the main channel of Pt–HMOR, molecular mechanics energy profiles for *n*-butane migration were calculated using MSIs Diffusion strategy [5]. This procedure performs constrained minimizations of the sorbed molecule along a previously defined path within the host structure. The host lattice is held rigid during the optimizations (Fig. 1).

The difference between the energies of *n*-butane at the minimum and the maximum along a minimum energy path between two nearest neighbor minima (binding sites), is quantified. From these calculations, a rough estimate of the accessibility of Pt sites for *n*-butane diffusing from the vacuum side into the Pt–HMOR pores, is to be expected. We have, then, calculated the diffusion for several possible paths into the main channel. Hence, no attempt has been made to determine the saddle point for *n*-butane adsorption into the model Pt–HMOR catalyst.

3. Results and discussion

3.1. Sorption of n-butane in a low-dispersed Pt–HMOR model catalyst

This section presents the modelling results of adsorption behavior of *n*-butane in Pt–HMOR, model 20. Such a Pt cluster of about 0.8 nm in size is consistent with transmission electron micrographs results for a 0.1–1.0 wt% Pt–HMOR catalyst [14].

In Table 2, both the MC sorption energies and the discover optimized values for the four lowest *n*-butane/Pt_{22}–HMOR configurations are displayed. In the minimum energy structures, *n*-butane meets isolated Pt sites inside the

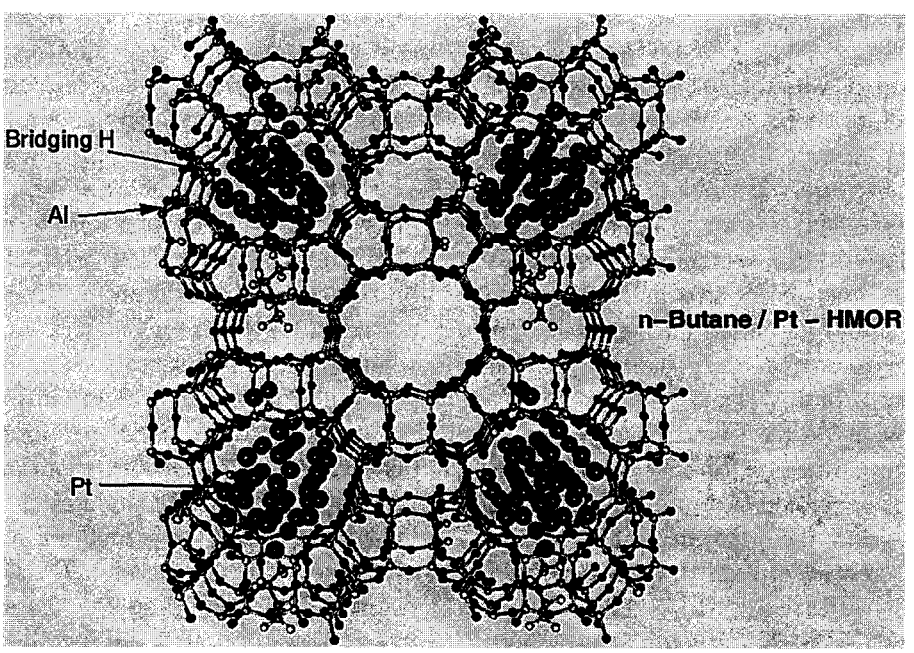

Fig. 1. Schematic diagram of the minimum energy structure of the *n*-butane/Pt_{22}–HMOR model system (see Table 2).

Table 2
Monte Carlo interaction energy values (kcal/mol), E_{MC}, and optimized lattice energies, E, for the four lowest sorption sites of n-butane in Pt_{22}/HMOR. PMS and FR refer to the partially minimized (Pt-cluster + n-butane) and fully relaxed (framework + Pt-cluster + n-butane) structures, respectively

Structure	E_{MC}	E	
		PMS	FR
1	68.2	−2596.7	−3419.5
2	100.8	−2573.5	−3820.3
3	106.8	−2585.9	−3388.4
4	110.0	−2530.7	−3337.3

mordenite side pocket, as expected from the pore blocking effect by this large Pt aggregate. The large steric hindrance for the adsorption of n-butane inside the Pt_{22}–HMOR pores is reflected in the repulsive MC interaction energy values (see Table 2). The stabilization gained relaxing the n-butane into the host structure and the subsequent optimization of the whole Pt_{22}–HMOR lattice overcompensates steric repulsions. Thus, the obtained lattice energies for the sorbed n-butane/Pt_{22}–HMOR systems are more negative (stable) than the starting host lattice.

Examination of the components to the total energy of the optimized structures reveals that the gain in attractive vdW dispersive contribution is responsible for the lattice energy lowering. This indicates that the n-butane molecule optimizes its vdW contacts with the zeolitic environment. This adsorbate self-organization on the substrate has been observed in several examples of confined reactants inside microporous catalysts, e.g. aromatization of n-hexane on (Ba, K)-exchanged zeolite L-based catalysts [15] and isomeric butenes in ZSM-5 [6].

The inclusion of the host framework relaxation in the minimization stage shows up to contribute importantly to the final sorbate binding energy (Table 2). In this stage of the minimization, the reduction of the vdW repulsive contribution is controlling the total energy lowering. This indicates that the host structure relaxes to accommodate the guest molecule reducing, in this way, steric repulsions.

From these results, the conclusion to be drawn is that under thermodynamic control, the active sites for n-butane adsorption might be isolated Pt atoms in the side pockets. Moreover, from experimental studies, the isolated Pt atoms in the mordenite side pockets have already been proposed as the active sites for the methylcyclopentane ring-opening [16]. However, care should be taken when interpreting this result, since the critical diameter for linear alkanes was calculated to be 0.45 nm [17], which is larger than the entrance dimension of the pocket (0.39 × 0.57 nm) and hence, Pt sites in the side pockets must be difficult to reach by the n-butane molecule.

3.2. *Sorption on highly dispersed Pt–HMOR model catalysts*

In this section, the simulation results of the sorption of butane and butene isomers in model Pt–HMOR catalysts are presented. These small Pt clusters provide accessible Pt sites in the main channel for n-butane adsorption, as well as monatomic sites in the side pockets. Table 3 displays the lowest MC interaction energies of the isomerization products relative to the reactant n-butane inside the Pt–HMOR model structures 6 and 4 calculated at an energy threshold of 773 kcal/mol.

In contrast to the large Pt cluster model 20, the lowest energy sorption sites for small cluster models are found to be located in the main channel. The relative MC interaction energies of the lowest energy docked conformations (Table 3) seem to indicate that an increase in the number of Pt sites in the main channel improves

Table 3
Relative Monte Carlo interaction energy values (kcal/mol)in Pt–HMOR

Isomer	Model 6	Model 4
n-butane	0	0
iso-butane	0.46	−0.12
butene	1.10	−0.02
iso-butene	−1.51	1.75

Table 4
Relative minimum binding energy values (kcal/mol) in the considered Pt–HMOR

Isomer	Model 6	Model 4
n-butane	0	0
iso-butane	−6.61	−6.61
butene	50.36	−8.05
iso-butene	45.82	−10.58
trans-but-2-ene	−1.12	−6.15
cis-but-2-ene	50.27	−6.79

the *iso*-butane and butene production, with a simultaneous lowering of the *iso*-butene yield over Pt–HMOR. As shown below, however, full energy relaxation of the low energy docked structures changes this tendency.

The minimum binding energies corresponding to the fully relaxed docked structures are listed in Table 4 (Fig. 2). As in Table 3, the isomer binding energies are given relative to the value for *n*-butane. An acceptance/rejection choice of 0 kcal/mol was made to avoid any docked conformation with steric hindrance. In this way, a more effective sampling of low energy sorption sites in the channel compared to a threshold of 773 kcal/mol can be performed prior to energy optimization.

Table 5
Optimized adsorption energies (kcal/mol) and location of *n*-butane in Pt–HMOR model catalysts

Model	20	6	4
E_a	−446.2	−20.1	−3.3
Location	side pocket	main channel	main channel

Upon relaxation, the lower the Pt dispersion in the main channel, the more strongly bound the *n*-butane is with respect to the isomeric butenes and *iso*-butane. *iso*-butane is the most strongly bound and its binding energy is the less affected by a change in the number of Pt sites. This result suggests an enhancement of the catalytic performance towards butene isomers with increasing metal particle size in the channel.

Table 5 summarizes the *n*-butane adsorption energies on all the considered Pt–HMOR models. The adsorption energy is calculated as the difference between the energies of the adsorbed system (*n*-butane/Pt–HMOR) and the separated *n*-butane and Pt–HMOR structures. The *n*-butane adsorption energy increases with the number of Pt atoms in the main channel. In the case of a large Pt cluster which effectively blocks the main channel, the only Pt sites avail-

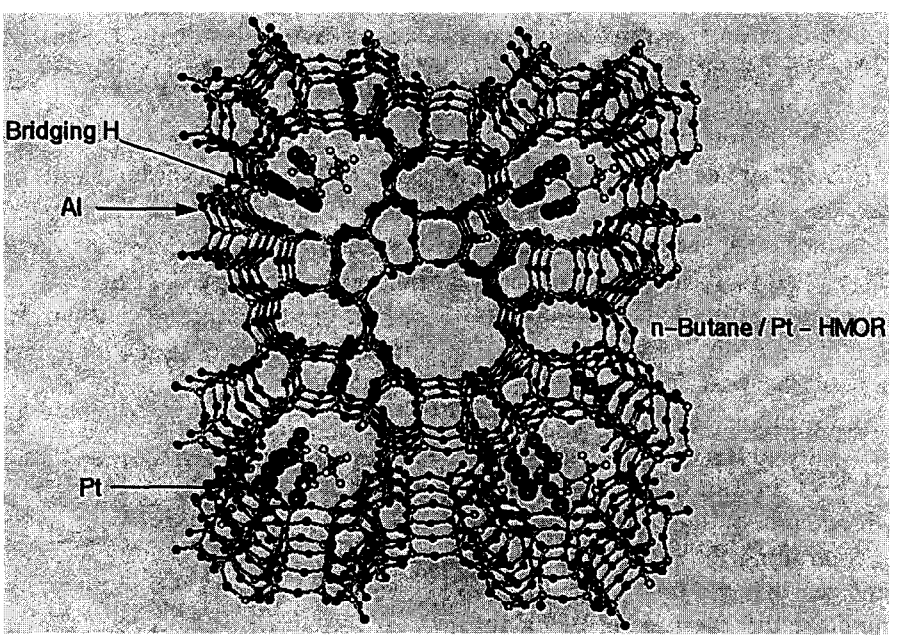

Fig. 2. Schematic diagram of the minimum energy structure of the *n*-butane/Pt_5HMOR model system (see Table 4).

able for *n*-butane adsorption are located in side pockets. In these small pores, the *n*-butane molecule optimizes more effectively its dispersive interactions with the pore walls. In the case of small Pt clusters in the main channel, on the other hand, the gain in *n*-butane adsorption energy with the number of Pt atoms is governed by a gain in attractive dispersive forces as the number of Pt atoms increases.

Previous Monte Carlo simulations of methane adsorption in faujasite, mordenite and ZSM-5, explained the high experimental heat of adsorption of methane in mordenite as compared to faujasite on the basis of the location of low energy sorption sites inside the side pockets [18].

The calculated change in the relative adsorption strength of *iso*- and *n*-alkanes (Table 4) might be relevant in interpreting the observed experimental increase in selectivity to light isomers with the platinum concentration [4]. On this catalyst, the alkane is dehydrogenated on metal sites, and the alkenes so produced are easily desorbed and migrate to acid sites to be isomerized (or cracked). The new *iso*-alkenes are later hydrogenated on metal sites or desorbed. Therefore, rising the Pt concentration, the possibility of alkenes to be isomerized, and subsequently hydrogenated, increase. This enhances, thus, the probability of *iso*-alkanes to be desorbed from the catalysts. This increase in selectivity to *iso*-alkanes is consistent with the observed parallel lowering in cracking products in the presence of more platinum, particularly because of the formation of the olefinic intermediates.

The resulting distances between the nearest

Table 6
Pt–H bond distances (Å) for a *n*-butane hydrogen atom, d_{Hb}, and the acidic proton, d_{Ha}, corresponding to the minimum energy *n*-butane adsorption configuration over the considered Pt–HMOR models

Model	4	6
d_{Hb}	2.54	2.53
d_{Ha}	1.93	2.19

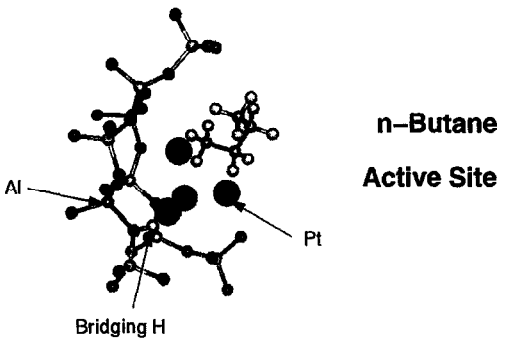

Fig. 3. Schematic diagram of the *n*-butane adsorption geometry in the Pt–HMOR main channel.

n-butane hydrogen atom to a hosted Pt site, as well as between a Brønsted mordenite proton to the nearest Pt atom are displayed in Table 6, for the calculated minimum adsorption sites of *n*-butane in the Pt–HMOR cluster models 6 and 4. The similarity between the optimized Pt–H distances for the two Pt–HMOR models is striking. In model 4, the four Pt atoms are arranged in a geometry similar to that of the hcp-hollow site in a (111) surface layer. The Pt–Pt distance of 2.86 Å in the supported cluster is close to value in a fcc-crystal. The *n*-butane adsorption geometry in Pt_5–HMOR (model 4) is shown in Fig. 3. The *n*-butane adsorption geometry over this Pt cluster resembles to that found by MD simulations at 50 K for *n*-butane physically adsorbed on a Pt(111) surface [19].

3.3. *n*-butane migration into Pt–HMOR

Different migration pathways from the vacuum into the Pt_7–HMOR main channel were calculated (model 6). In this section only two of the defined trajectories, involving the lowest differences between the energies of *n*-butane at the minimum and at the maximum along the associated path, are presented. The minimizations entail relaxation of the *n*-butane at constrained points, in steps of 0.2 Å, along the path.

A trajectory of 10 Å along the main channel was defined in a Pt_7–HMOR molecule containing 465 atoms. *n*-butane diffusing along this trajectory from the vacuum inside the mordenite

main channel, migrates first to a minimum energy site in the side-pocket and finds subsequently a second stable sorption site, in the main channel. The obtained energy difference of 40.0 kcal/mol between the two minima is quite large, which might prevent the interaccessibility of both minimum energy sites within the pore structure. Certainly, reliable predictions on diffusion behavior are to be given by dynamical diffusion barriers, calculated taking into account temperature effects by molecular dynamics simulations and adopting a more realistic model, such as a flexible framework.

The lowest energy difference of 1.32 kcal/mol was calculated for a trajectory along the straight channel, which is quite low compared with $kT = 1.64$ kcal/mol at a typical reaction temperature of 550°C. This suggests that the Pt_7–HMOR channel structure might be energetically accessible by a *n*-butane molecule diffusing from the vacuum side. The eight-ring secondary pores are impassable by a single *n*-butane molecule migrating from the straight channels, at all the defined trajectories, as suggested by the large energy differences obtained.

4. Conclusions

A variety of simulation techniques have been applied to address the structure-selectivity relationship in the hydroisomerization/dehydrogenation reaction of *n*-butane in the bifunctional catalyst Pt–HMOR. Thereby, it is evidenced that the pore structure of mordenite not only affects the size and location of Pt particles, but also provides molecular sieve properties for the intermediates and products to be formed selectively in the reactions.

At high Pt loading levels, the active sites are isolated Pt atoms nearby side pockets. The preferred hydrocarbon location in mordenite loaded with metal at high dispersion are Pt sites in the straight channels.

The presence of active sites in side pockets at high metal content gives rise to a significantly higher *n*-butane binding energy. In the small pores, the adsorbate makes a more beneficial profit of its vdW dispersive interactions with the zeolite walls.

The trend observed at high metal dispersion in the change of the relative binding energies of *n*-butane compared to the isomers with the size of the Pt particles in the main channel, is of significance for the *n*-butane hydroisomerization reaction in Pt–HMOR.

Acknowledgements

The authors would like to acknowledge T. Romero for useful discussions and thank INTEVEP S.A. for permission to publish this work.

References

[1] R.A. Asuquo, G. Eder-Mirth and J.A. Lercher, J. Catal. 155 (1995) 376.
[2] F. Eder, M. Stockenhuber and J.A. Lercher, in: Zeolites: A Refined Tool for Designing Catalytic Sites, L. Bonneviot and S. Kaliaguine (Eds.), Elsevier, 1995, pp. 495–500.
[3] J.C. Yori, M.A. Dámato, G. Costa and J.M. Parera, React. Kinet. Catal. Lett. 56 (1995) 129.
[4] J.M. Grau and J.M. Parera, Appl. Catal. A 106 (1993) 27.
[5] Catalysis package, version 2.3.7 (Molecular Simulations Inc., 1995).
[6] C.M. Freeman, C.R.A. Catlow, J.M. Thomas and S. Brode, Chem. Phys. Lett. 186 (1991) 137.
[7] Discover molecular simulation program, version 94.1 (Molecular Simulations Inc., 1995).
[8] J.D. Doll and H.K. McDowell, J. Chem. Phys. 77 (1982) 479.
[9] J.D. Doll and H.K. McDowell, Surf. Sci. 123 (1983) 99.
[10] H.K. McDowell and J.D. Doll, J. Chem. Phys. 78 (1983) 3219.
[11] J.D. Doll and D.L. Freeman, Surf. Sci. 134 (1983) 769.
[12] S.M. Levine and S.H. Garofalini, Surf. Sci. 163 (1985) 59.
[13] M.E. Grillo and M.M. Ramírez de Agudelo, J. Mol. Model. (1995), submitted.
[14] G. Giannetto, A. Montes, F. Alvarez and M. Guisnet, Rev. Soc. Venez. Catal. 5 (1991) 33.
[15] E.G. Derouane and D.J. Vanderveken, Appl. Catal. 45 (1988) L15.
[16] G. Lei and W.M.H. Sachtler, J. Catal. 140 (1993) 601.
[17] E.G. Derouane, Intercalation Chemistry (Academic Press, New York, 1984).
[18] B. Smit and C.J.J. den Ouden, J. Phys. Chem. 92 (1988) 7169.
[19] K.A. Fichthorn, P.G. Balan and Y. Chen, Surf Sci. 317 (1994) 37.